Abstracts for the Fourteenth International Conference on the Application of Accelerators In Research & Industry November 6, 7, 8, and 9, 1996

University of North Texas
Department of Physics
Denton, Texas, USA

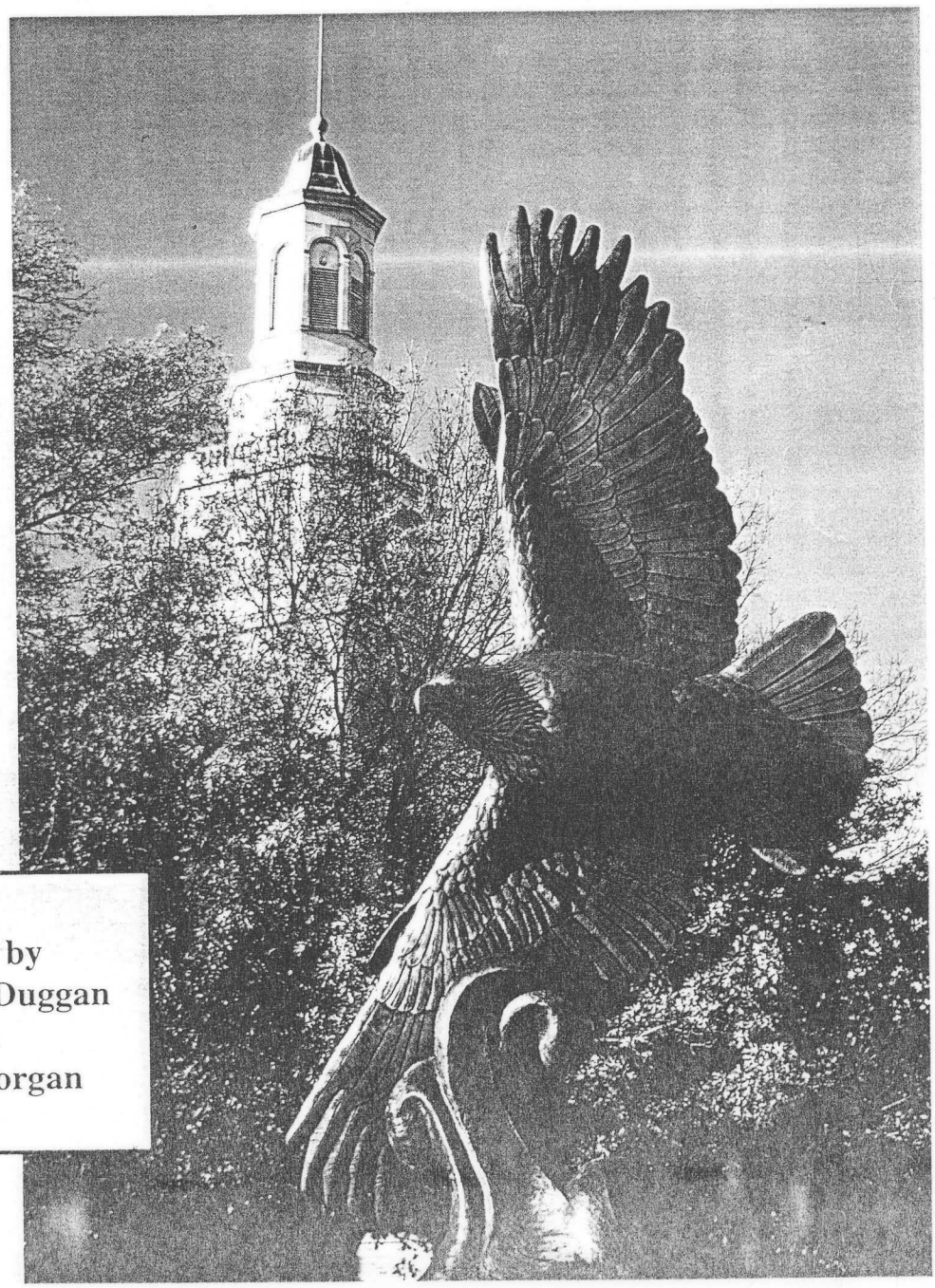

Edited by
Jerome L. Duggan
and
I. Lon Morgan

FC6 INVITED POSTER PAPER: See Poster Display PB38

Lateral and Depth Distribution of Hydrogen in Poly-crystalline Silicon Solar Cells. **(5 min.) at 20:35**

C.L. CHURMS, V.M. PROZESKY, T.K. MARAIS, R. PRETORIUS, *Van de Graaff Group, National Accelerator Centre, Faure, South Africa,* J. VAN DER WEG, *Debye Institute, University of Utrecht, The Netherlands*, and W. SIMKE, *Energie Ondersoek Centrum, Nederland, Petten, The Netherlands*.

The use of hydrogen as passivator is well known in silicon solar cells. The function of the hydrogen is to occupy the available states in the silicon by fixing the dangling bonds that normally occur at defects, such as dislocations and grain boundaries in the silicon. In this study we used the micro-ERDA (Elastic Recoil Detection Analysis) technique to determine the lateral and depth distribution of the hydrogen in poly-crystalline solar cells. To discriminate against atmospheric influences, the solar cells were manufactured with deuterium as passivation. The ability of ERDA, using ^{4}He as primary ions, to discriminate between hydrogen and deuterium signals enabled us to study both the passivation effect of deuterium and atmospheric affects of hydrogen. The distribution of deuterium was found not to peak at the grain boundaries of the individual single crystals, but to be homogeneously distributed in the single crystals, although some crystals did tend to have higher concentrations of deuterium than others.

FD SESSION: ATOMIC PHYSICS AND RELATED PHENOMENA

Thursday evening, 7 November 1996; University Union, Room 412 at 18:30

J. FEAGIN, California State University, presiding

FD1 **Measurements of L-Subshell Ionisation Cross Sections of Ho, Er, and Tm by α-Particle Bombardments.** **(20 min.) at 18:30**

B.A. SHEHADEH[1], A.B. HALLAK[2], and M.A. GARWAN[1], [1]*Physics Department, KFUPM, Dhahran 31261, Saudi Arabia,* [2]*Physics Department, Al-Albyte University, Maffraq, Jordan.*

The L-Subshell ionisation cross sections induced by 1-6 MeV α particles are measured experimentally for Ho, Er, and Tm. The experimental data are compared with the theoretical predictions of the ECPSSR theory. Fair agreement is found for the L_3 subshell, whereas considerable disagreements are noticed for the other two subshells in particular the L_2 subshell. Possible reasons for the discrepancies are discussed.

FD2 **Classical and Quantal Aspects of Electron Transfer Processes in Ion-Atom Collisions.*** **(20 min.) at 18:55**

A. DUBOIS, *Laboratoire de Chimie Physique-Matiere et Rayonnement, Paris, France.*

The development of new sophisticated experimental technics has allowed the understanding of electronic processes occurring during atomic collisions at levels never reached in the past. For example, in ion-atom collisions, studies of the dynamics of oriented and aligned states provide detailed confrontations between experiments and theories and thus permit severe tests of the models.[1] In this context, comparisons between xperiments, quantal and classical approaches will be presented for electron transfer in intermediate impact energy collisions. Especially, the quantal approach, the semiclassical atomic close coupling model combined with the eikonal approximation, will be compared with the classical trajectory Monte Carlo (CTMC) method. The discussion will be illustrated for the dominant electron transfer channels in *planar* H^+-$Na(3p_{\pm1})$ collisions[2]. The theoretical models will be confronted for nlm-state resolved impact parameter probabilities and comparisons with experimental data[3] will be provided by differential cross sections. It will be shown that, though significative quantitative discrepencies exist at these energies, the CTMC method gives good agreement with quantal results when considering orientation effects.

*Unité associée au CNRS URA 176, Université Pierre et Marie Curie, 11, rue Pierre et Marie Curie, F-75231 Paris Cedex 05, France.

[1]N. Andersen, in Proceedings of the Eighteenth ICPEAC, Aarhus, Denmark (AIP Press, New York), 505 (1993).
[2]A. Dubois and J.P. Hansen, J. Phys. B, 29, L225 (1996).
[3]C. Richter, N. Andersen, J.C. Brenot, D. Dowek, J.C. Houver, J. Salgado and J. Thomsen, J. Phys. B26, 723 (1993).

FD3 **Electron Detachment from H^- by Fast Protons and Electrons.** **(20 min.) at 19:20**

D. BELKIĆ, *Stockholm University, Stockholm, Sweden.*

Unexplained for some 20 years, a flagrant disagreement by two orders of magnitude has existed between the eikonal Coulomb Born (ECB) approximation[1] and the experiment[2] on total cross sections for the electron detachment process $H^+ + H^- \rightarrow H^+ + H + e$. We show that this is due to inconsistency between the Coulombic distortion effects and the perturbing potential operator in the T-matrix of the ECB model. Moreover, the total cross sections σ of the ECB approximation tend to a constant value instead of the correct Bethe asymptote $\sigma \sim (1/E)\ln E$ as the incident energy E increases. These shortcomings of the ECB method are presently lifted altogether by properly connecting the initial and final scattering states with the perturbation interactions. Such an improvement yields good agreement with the experiments at high energies for both proton[2] and electron[3] impact detachments of H^-. In addition, we have studied the electron correlation effects in the bound state of H^- by using the 5-33 parameter Hylleraas-type wave functions of Rotenberg and Stein, as well as the 2-60 configuration interaction (CI) orbitals of Silverman, Tweed and Joachain. Great sensitivity of both differential and total cross sections to these electron correlations is found.

[1] R. Gayet, R.K. Janev and A. Salin, J.Phys.B **6**, 993 (1973).
[2] B. Peart, R. Grey and K.T. Dolder, J.Phys.B **9**, 3047 (1976).
[3] B. Peart, D.S. Walton and K.T. Dolder, J.Phys.B **3**, 1346 (1970).

FD4 **Quantum Description of Dechanneling by Extended Defects.** **(20 min.) at 19:45**

A.P. PATHAK and L.N.S. PRAKASH GOTETI, *School of Physics, University of Hyderabad, Central University P.O. Hyderabad - 500 046, India.*

A quantum description of the effects of extended defects on charged particle propogation in single crystals has been developed. We have considered stacking faults and dislocations as two examples. The stacking faults present mainly obstruction type effects and depending on the phase of approaching probe particles and amount of stacking shift the particle motion may be affected. The dislocations on the other hand produce distortion in the crystallographic channels and the effects depend directly on the magnitude of this distortion which depends upon the concentration

Measurements of the L-Subshell Ionisation Cross Sections of Ho, Er, and Tm by α-Particle Bombardments.

B. A. Shehadeh, A. B. Hallak and M. A. Garwan
Energy Resources Division, Research Institute,
King Fahd University of Petroleum and Minerals,
Dhahran 31261, Saudi Arabia

The L-subshell ionisation cross sections induced by 1-6 MeV α particles are measured experimentally for Ho, Er, and Tm. The experimental data are compared with the theoretical predictions of the ECPSSR theory. fair agreement is found for the L_3 subshell, whereas a considerable disagreements are noticed for the other two subshells in particular the L_2 subshell. Possible reasons for the discrepancies are discussed and final conclusion is presented.

1. Introduction

The rapid development and increasing availability of particle accelerators, as well as the development of quantum mechanics, have induced the scientists to pay more attention to ion-atom collision in both experimental and theoretical points of view. Nowadays, most of the studies are directed towards explaining and predicting the experimental results of ion-atom collision. One of the important consequences of ion-atom collision is the ionization of inner-shell electrons, that produces characteristic X rays. This effect is mainly utilized in wide applications, specifically, basic research of quantum collision theories, X-ray production, and material science. Since we have mainly collision phenomena, the important physical quantity, through which the nature of collision can be understood, is the cross section. More recently, many attempts have been made to measure the ionization cross sections by light ion impacts experimentally and compare them with the available theoretical predictions.

In this study the L subshells ionization cross sections by α-particle bombardments are measured for three elements of the rare earth group, namely, holmium, erbium, and thulium. The study is an advanced attempt after appreciable studies for the K-shell and the L-subshell ionization cross sections by proton bombardments. The study of L-subshell ionization by α particles is selected because most of the theoretical and experimental studies have dealt with the K shell. This lack of attention paid to L shell is due to its greater complexity from both experimental and theoretical points of view. Since the L shell consists of three degenerate or nearly degenerate subshells, L_1, L_2, and L_3 subshells with particular atomic parameters for each. Furthermore, studying L subshells by α particles offers a data base to test the validity of first order theories to draw a clear conclusion and obtain evident understanding for ion-atom collision since up to now, the experimental data for such study are far from sufficient[1].

In the present paper the experimental results of the L-subshell ionisation cross sections of Ho, Er, and Tm induced by 1-6 MeV α particles are presented. The measured data are compared systematically with the ECPSSR predictions.

2. Experimental Procedure

The α beam is obtained from duoplasmetron-type ion source and then accelerated, transported, and focused via 3 MV General Ionix Tandetron accelerator of Energy Research Laboratory (ERL) at KFUPM Research Institute. The various sectors of the accelerator are described in details elsewhere[2]. The shaped beam was directed towards the target in PIXE/RBS scattering chamber. The chamber was made of aluminium and installed as an automated RBS/PIXE chamber with a remotely controlled goniometer. A schematic diagram for the chamber setup is shown in figure (1).

The Si(Li) detector was brought as close as possible to the target (11 cm) by means of a stainless steel well with a window at the end close to the detector. The window was made from Kapton foil of 63 μg/cm^2 thickness which allows soft X rays to pass through and at the same time withstands repeated venting and pumping of the chamber to a pressure of about 10^{-6} torr[3]. An external absorber, is used to attenuate low energy X rays, was constructed from graphite. A hole of 1 mm in diameter constrains the majority of X rays photons to incident on the active area of Si(Li) detector crystal to avoid the edge effects, which reduces the distortion in peak shaping and minimizes the tailing effect. Additionally, pinhole absorber reduces the bremsstrahlung by secondary electrons that appears at low energy region. The typical resolution of Si(Li) detector is 190 eV for Mn K_α line. The goniometer is controlled by IBM PC computer and equipped with precise stepper motor for controlling the position of the sample holder in three dimensions. The same computer is interfaced to a Nuclear Data ND62 multi-channel analyser which is used

Figure 1. Schematic diagram shows the *PIXE/RBS* setup at the Tandetron accelerator laboratory.

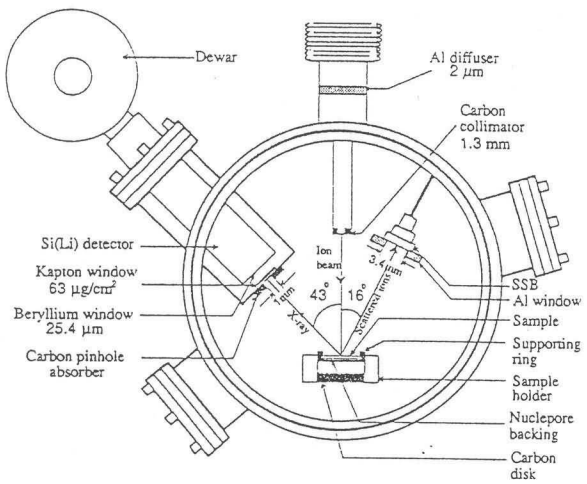

Figure 2. The X-ray spectrum produced by 6 MeV α-particle bombardments on Tm.

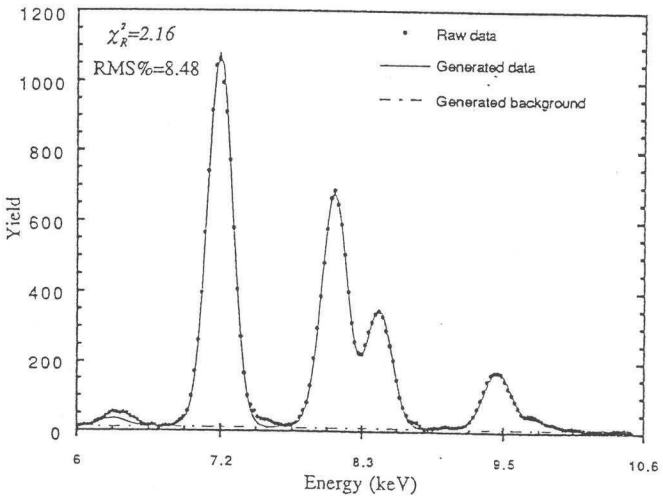

with the computer for data acquisition and analysis. With the presence of surface barrier detector (typical resolution is 16 keV for ^{241}Am $E_\alpha = 5.486$ MeV), the system, therefore, implements simultaneous analysis of PIXE and RBS. The collected charges were integrated by the Ortec digital current integrator. The number of α particles which hit the target was determined by considering the backscattered α particles.

Thin film standards (Provided by MICROMATTER Co. USA.) are employed for this study. The samples and their areal density are HoF_3 (37.4 μg/cm^2 for Ho), ErF_3 (36.8 μg/cm^2 for Er), and TmF_3 (37.4 μg/cm^2 for Tm). The purity, dimensions, and shapes of standards were achieved under a certain restrictions required for convenient determination. These standards are prepared by vacuum deposition resulting in highly uniform deposit. In most cases the standards present an element free of interfaces and thin enough to ignore thickness effects, which makes the analysis easier. The elements are deposited onto 25 mm-diameter Nuclepore polycarbonate membrane filter (approximately 1mg/cm^2 thick), and mounted by 1 mm-thick polycarbonate rings. The uncertainty in the thickness was estimated by the manufacturer to be within $\pm$0.5%. The samples were irradiated by 1-6 MeV α particles by a beam current was limited to 1-3 nA to avoid pile-up and dead time effect.

In order to deduce the L-subshell ionisation cross sections, the peak areas of $L_{\alpha_{1,2}}$, L_{β_1}, and $L_{\gamma_{2,3}}$ lines were calculated using the least-square-fitting program BATTY of the PIXAN-PC package[4]. For a given element, the package was modified to fit the X-ray lines of each subshell independently in order to avoid the energy dependence of the relative intensities among different subshells. The relative intensities of each subshell lines are taken from the experimental values of Salem *et al.*[5].

3. Results and Discussion

The X-ray production cross section for a thin target yields were calculated as

$$\sigma_s^x(E) = \frac{4\pi}{\varepsilon}\frac{\Omega'}{\Omega}\frac{N_s^x}{N^\alpha}\left(\frac{d\sigma}{d\Omega}\right)_R, \qquad (1)$$

where N_s^x and N^α are the X-ray yield of the S subshell (S stands for L_1, L_2, and L_3) and backscattered α-particle yields, $(d\sigma/d\Omega)_R$ is the differential Rutherford backscattering cross section, Ω' and Ω are the solid angles subtended by the surface barrier and Si(Li) detectors, respectively, and ε denotes the efficiency of the Si(Li) detector. The advantage of thin target measurements is the possibility of utilizing both PIXE and RBS simultaneously. Thus, the accumulated charge and target areal density are irrelevant in the calculations which improves the accuracy of the measurements. This shows why it is favourable to use thin targets in such measurements rather than thick targets.

For the K-shell ionization cross sections by proton bombardment, the ECPSSR theory provides values agree with the experimental data within $\pm$6%[6,7]. Thus, we utilized this attribute to normalize equation

Figure 3. The principal L X-ray lines for Tm, after separating the unresolved lines using Gaussian line shape model.

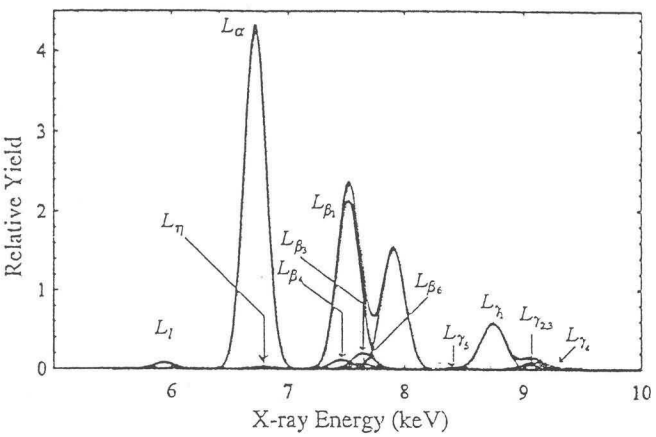

(1) for the efficiency-geometry factor $\{(1/\varepsilon)(\Omega'/\Omega)\}$ of our system. The peak areas N_K^x, as well as N^p, are obtained for K-shell ionization induced by 2.5 MeV protons incident on a set of thin films for a various elements whose Z ranging from 17 to 41. The reason of choosing 2.5 MeV protons is that the energy dependence of the cross sections for these elements exhibit a broad maxima around 2.5 MeV. Therefore, small deviations in the energy of the proton beam does not alter the values of the cross sections or peak areas significantly. Additionally, the X-ray spectra induced by 2.5 MeV protons for these elements have high detection sensitivity[8]. Therefore, high X-ray yields can be achieved which reduces the statistical fluctuations of the PIXE spectra and consequently more precise peak areas can be obtained. For K-shell ionization, the ECPSSR values of Cohen and Harrigan[9], the fluorescence yields of Krause[10], and the relative intensities of Salem *et al.*[5] are adopted and an analytical expression for the efficiency-geometry factor as a function of X-ray energy was obtained. The energy dependence of the efficiency-geometry factor is a consequence to the energy dependence of the efficiency. The uncertainty in the efficiency-geometry factor was estimated to be within $\pm 6.8\% - 7.4\%$.

The yields of L_α, L_{β_1}, and $L_{\gamma_{2,3}}$ were employed to obtain the production cross sections for L_1, L_2, and L_3 subshell, respectively. The yield of each X-ray line was converted into subshell yield, N_{L_i}, by dividing it by the branching ratio, i.e.

$$N_{L_1} = \frac{L_{\gamma_{2,3}}}{B_{L_{\gamma_{2,3}}}}\ ;\ N_{L_2} = \frac{L_{\beta_1}}{B_{L_{\beta_1}}}\ ;\ N_{L_3} = \frac{L_\alpha}{B_{L_\alpha}}, \qquad (2)$$

where

$$B_{L_{\gamma_{2,3}}} = \frac{\Gamma_{L_{\gamma_{2,3}}}}{\Gamma_{L_1}}\ ;\ B_{L_{\beta_1}} = \frac{\Gamma_{L_{\beta_1}}}{\Gamma_{L_2}}\ ;\ B_{L_\alpha} = \frac{\Gamma_{L_\alpha}}{\Gamma_{L_3}} \qquad (3)$$

and $\Gamma_{L_i} = \sum_{j=1}^{N} \Gamma_j$, the total L_i subshell emission rate ($i = 1$, 2, and 3). The values of the branching ratios were taken from the experimental values of Salem *et al.*[5].

If the vacancy migration effect for a vacancy created in the K shell is neglected[11] the direct ionization cross section for L_1, L_3, and L_3 subshells are given by, respectively

$$\sigma^i_{L_1}(E) = \frac{\sigma^x_{L_1}(E)}{\omega_{L_1}}, \qquad (4)$$

$$\sigma^i_{L_2}(E) = \frac{\sigma^x_{L_2}(E)}{\omega_{L_2}} - f_{12}\sigma^i_{L_1}(E), \qquad (5)$$

and

$$\sigma^i_{L_3}(E) = \frac{\sigma^x_{L_3}(E)}{\omega_{L_3}} - f_{23}\sigma^i_{L_2}(E) - (f_{13} + f_{12}f_{23})\sigma^i_{L_1}(E), \qquad (6)$$

where ω_{L_i} is the L_i-subshell fluorescence yield, and f_{ij} denotes the Coster-Kronig transition probability between L_i and L_j subshells.

The values of the ionization cross sections are very sensitive to the adopted decay parameters (fluorescence yields and Coster-Kronig transitions)[12]. Therefore, it is interesting to use the two tribute data sets for the atomic decay parameters, those are the semi-empirical values of Krause[10] and the theoretical values of Chen *et al.*[13]. This is to compare the behaviour of the ionization cross section at two different data sets of decay parameters, and to find a reason for any possible discrepancy.

The measured L-subshell ionization cross sections and the ECPSSR calculations of Ho, Er, and Tm are shown graphically as a functions of the energy of the projectile in figures (4), (5), and (6), respectively. For the three elements, the general tendency of the ionization cross sections is similar. The solid points represent the ionization cross-section values those were calculated by adopting the atomic decay parameters of Krause, whereas the hallow points represent that the ionization cross-section values that were calculated by adopting the atomic decay parameters of Chen *et al.* The curves in the plots represents the ECPSSR predictions taken from Cohen and Harrigan[9]. The reason of choosing this version of the ECPSSR is due to the accurate estimations of the integration limits of the form factor and correction factors and detailed tabulated cross-section

Figure 4. A plot of the L_1, L_2, and L_3-subshell ionization cross sections for Ho by α-particle bombardment, versus α-particle bombardment energies. The curves represent the predictions of the ECPSSR theory.

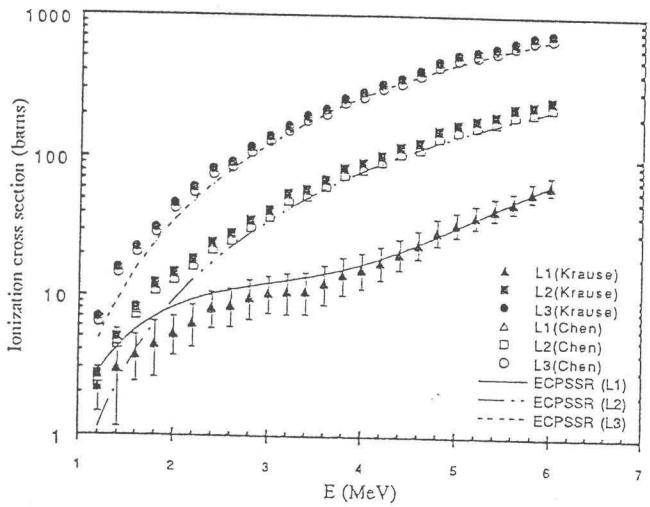

values at various bombardment energies of α particles. The error bars in the figures demonstrate the contributions of the uncertainties of the peak areas and the efficiency-geometry factor, neglecting the contributions of the atomic decay parameters adopted in the calculations.

Except L_1 subshell, the experimental values which were calculated by adopting the theoretical decay parameters of Chen *et al.* are lower and closer to the theoretical predictions than those were calculated by adopting the semi-empirical decay parameters of Krause. However, the theoretical predictions underestimate the experimental values for L_2 and L_3 subshells for the three elements when the bombardment energy is less than 4 MeV and discrepancies increase as the energy decreases. This agrees with the general results of most of the literatures[14–16]. However for L_1 subshell, the theoretical predictions over estimate the experimental ionization cross sections when the bombardment energy is less than 4 MeV whereas a satisfactory agreement between theory and experiment at energies higher than 4 MeV turns up. The trend of L_1 subshell experimental cross sections with respect to the theoretical predictions is similar to that given by Cuzzocrea *et al.*[17].

A possible conclusion from above discussion and from figures (4-6) is that the L_2 and L_3-subshell ionization cross sections increase on the expense of L_1-subshell ionization cross section. This can be explained in accordance to the effect of collision-induced intra-shell

Figure 5. A plot of the L_1, L_2, and L_3-subshell ionization cross sections for Er by α-particle bombardment, versus α-particle bombardment energies. The curves represent the predictions of the ECPSSR theory.

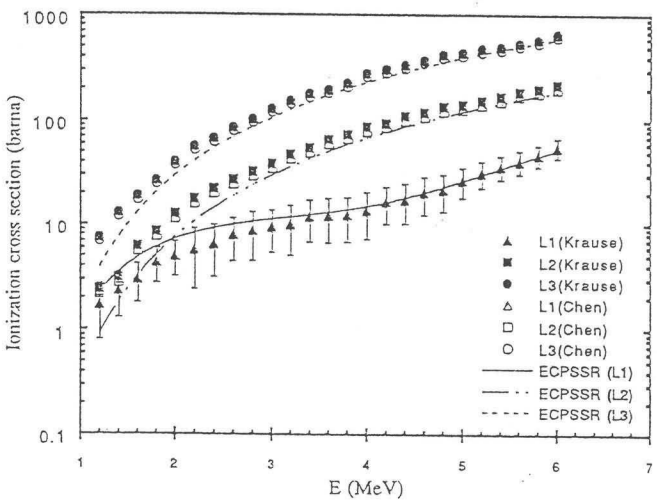

Figure 6. A plot of the L_1, L_2, and L_3-subshell ionization cross sections for Tm by α-particle bombardment, versus α-particle bombardment energies. The curves represent the predictions of the ECPSSR theory.

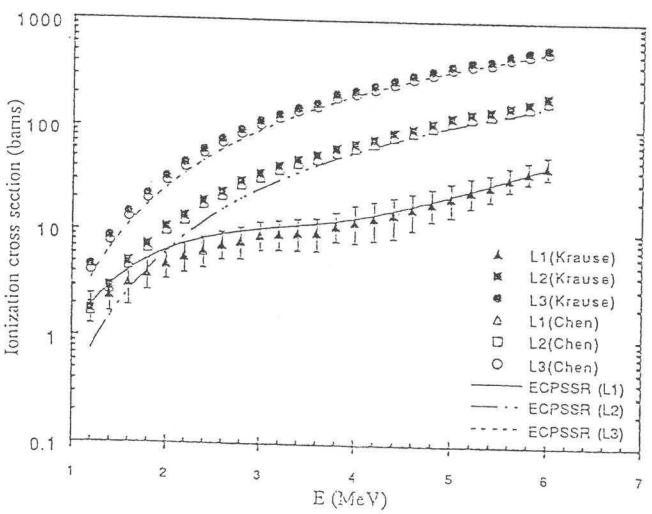

transition introduced by Sarkadi and Mukoyama[12,16]. Additionally from the figures (4-6), the extrapolation of the experimental values at energies less than 1.2 MeV shows that $\sigma^i_{L_1} > \sigma^i_{L_2}$. This is predicted by the ECPSSR theory but at energies less than 2 MeV. This can be explained in view of binding effect. This effect at low energy α particles becomes much larger for L_2 subshell than L_1 subshell since the response time (inversely proportional to electronic binding energy) of L_2 subshell electron is much longer than the collision time compared with L_1 subshell electron, that suppresses the ionization cross section of L_2 subshell significantly and raises this circumstance[18]. The binding effect no longer holds at high energies since the collision time is very short compared to the electronic response time in any particular subshell.

For the sake of proper analysis, the experimental ionization cross sections must be normalized by the theoretical predictions of the ECPSSR and plotted versus relevant scaling parameter. In this case, the parameter is selected to be the reduced velocity parameter ξ_{L_i} which is given according to Basbas *et al.*[19] as

$$\xi_{L_i} = \frac{2Z_{2L}}{n^2 I_{L_i}} \sqrt{\frac{m}{M_1} R_\infty E}, \qquad (7)$$

where E and M_1 are the energy and mass of the projectile, respectively, n is the principal quantum number ($n = 2$ in the present case), I_{L_i} is the experimental binding energy, and Z_{2L} is the effective nuclear charge of the target atom ($Z_{2L} = Z_2 - 4.15$). The parameter ξ_{L_i} was chosen because it gives the characteristic of a particular shell at certain bombardment energy. Moreover, one becomes able to distinct between the fast and slow collisions according to the demarcation of Basbas *et al.*[19]. In recent works, the parameter ξ_{L_i} is usually replaced by the relativistic reduced velocity parameter $\xi^R_{L_i}$ which is related to ξ_{L_i}. However, one is not concerned in reducing the statistical fluctuations of the normalized data points, but in contrast to verify any possible discrepancies in order to come up with rigorous conclusions.

Figure (7) shows the ratio $\sigma^{\exp}_{L_i}/\sigma^{ECPSSR}_{L_i}$ versus the reduced velocity parameter ξ_{L_i} of α-particle impact for L_1, L_2, and L_3 subshells, respectively. For L_1 subshell, the ECPSSR theory over estimates the experimental points when $\xi_{L_1} < 0.27$ and average deviation is estimated to be 27% within this range for all points either calculated by the decay parameters of Krause or Chen *et al.* When $\xi_{L_1} > 0.27$, the points start improving and an average deviation around $\pm 3\%$ is estimated for the points which were calculated by the decay parameters of Krause, and $\pm 2.6\%$ for the points which were calculated by the decay parameters of Chen *et al.*

In case of L_2 subshell the ECPSSR theory underestimates the experimental data up to factor 3. The

Figure 7. The ratio $\sigma^{\exp}_{L_i}/\sigma^{ECPSSR}_{L_i}$ versus the reduced velocity parameter ξ_{L_i} for α-particle induced L_1, L_2, and L_3-subshell ionization. Each element is marked by a different symbol (see legend). Dark symbols indicate that the decay parameters of Chen *et al.* are adopted and open symbols indicate that the decay parameters of Krause are adopted.

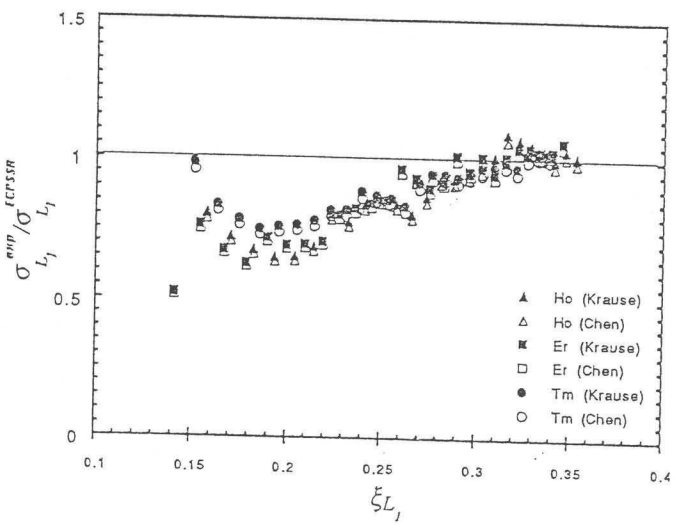

discrepancies decrease gradually with increasing the reduced velocity. Improvement starts within the range $\xi_{L_2} > 0.28$, in which average deviation is estimated to be 7% for the points that were calculated by the decay parameters of Chen *et al.* and 16% for the points those were calculated by the decay parameters of Krause. Whereas a 29% and 36% average deviations are estimated for the experimental values that were calculated by Chen *et al.* and Krause, respectively, when $\xi_{L_2} < 0.28$. A similar general tendency is observed for the L_3 subshell. However, here the experimental results agree much better with the theory. The theory also underestimates the experimental values up to factor 1.8. The average deviation is estimated to be 17% and 23% for the experimental values that were calculated by Chen *et al.* and Krause, respectively, at $\xi_{L_3} < 0.30$, while a 3.9% and 10.5% average deviations from the theory are estimated for the experimental values that were calculated by Chen *et al.* and Krause, respectively, when $\xi_{L_3} > 0.30$.

One can generally conclude that there are fair agreements between the ECPSSR predictions and experimental values especially at low energies and the strongest discrepancies between the experimental data and theoretical predictions are found for the L_2 subshell. One claim, that is also mentioned in many liter-

atures, is that the discrepancies are mainly due to the multi-vacancy configuration which alter the single-hole atomic decay parameters entirely. In multi-vacancy process, one expects that the detected X-ray lines to be broadened and comparable intensities of satellite lines are presented. These prospects were not detected in our experiment which not support such proclaims. Moreover, another test can verify whether the multi-vacancy effect holds or not, that is to estimate the relative intensities of the X-ray lines, those originated from a common subshell, and compare them with the corresponding single-vacancy relative intensity values of Salem *et al.*[5]. This is because when a multi-vacancy creation takes place, the relative intensities of X-ray lines are altered drastically and large departure from the relative intensity values that are produced by single-vacancy creation. It was found that the $L_{\beta_{2,15}}/L_{\alpha}$, L_{γ_1}/L_{β_1}, and $L_{\gamma_{2,3}}/L_{\beta_3}$ values for the three elements are constant with respect to the bombardment energies and agree well within the experimental errors with those values estimated by Salem *et al.* except for Tm $L_{\beta_{2,15}}/L_{\alpha}$, which is appreciably larger than the that of Salem *et al.* due to the overlapping of $L_{\beta_{2,15}}$ line with the γ rays induced by the ^{169}Tm-8.41 keV level[20]. The above argument implies that the multiple-vacancy effects are negligible. Therefore, it is favourable to modify the ECPSSR theory for the induced intra-shell transitions that favour vacancy transfer from the L_1-subshell to the L_2 and probably L_3-subshell following the recipe of Sarkadi and Mukoyama[12,16].

4. Conclusion

The L-subshell ionisation cross sections of Ho, Er, and Tm induced by 1-6 MeV α particles were measured experimentally using two sets of atomic decay parameters, those are the semi-empirical values of Krause[10] and the theoretical values of Chen *et al.*[13]. Comparing the data with the theoretical predictions of the ECPSSR, a general disagreement is observed especially at low bombardment energies. The discrepancy reaches its maximum for the particular subshell L_2. In general, the experimental cross sections which were estimated by adopting the theoretical atomic parameters of Chen *et al.* are closer to the predictions of the ECPSSR than those were calculated by adopting the decay parameters of Krause. The considerable disagreement of the experimental L_2-subshell ionisation cross sections with the ECPSSR theory suggests that the theory should be modified to account for the intra-shell transitions effect induced by the strong perturbational Coulomb field of α particles which favour vacancy transfer from the L_1 subshell to the L_2 subshell. It was found that the multiple-vacancy creations has a limited effect on the experimental measurements.

Acknowledgments

The authors acknowledge the support of The Energy Resources Division of The Research Institute, King Fahd University of Petroleum and Minerals.

REFERENCES

1. X. Cai, Z. Y. Liu, X. M. Chen, S. X. Ma, Z. C. Chen, Q. Xu, H. P. Liu, and X. W. Ma, *Nucl. Inst. Meth.*, **B72**(1992), 159.
2. H. Al-Juwair, M. M. Al-Kofahi, A. B. Hallak, and M. Rajeh, *Nucl. Inst. Meth.*, **B50**(1990), 474.
3. B. A. Shehadeh, *MSc Thesis*, 1994, King Fahd University of Petroleum and Minerals.
4. E. Clayton, P. Duerden, and D. Cohen, *Nucl. Inst. Meth.*, **B22**(1987), 64.
5. S. I. Salem, S. L. Panossian and R. A. Krause, *Atom. Data Nucl. Data Tables,* **14**(1974), 91.
6. H. Paul, *Nucl. Inst. Meth.*, **B4**(1984), 211.
7. H. Paul and J. Muhr, *Phys. Report,* **135**(1986), 47.
8. S. A. E. Johannson, and J. L. Campbell, *"PIXE: A Novel Technique for Elemental Analysis."* John Wiley & sons (1988), Chichester, UK.
9. D. Cohen and M. Harrigan, *Atom. Data. Nucl. Data Tables,* **33**(1985), 255.
10. M. O. Krause, *J. Phys. Chem. Ref. Data,* 8(1979), 307.
11. B. A. Shehadeh and A. Hallak, To be published.
12. L. Sarkadi and T. Mukoyama, *Phys. Rev.*, **A37**(1988), 4540.
13. M. H. Chen, B. Crasemann, and H. Mark, *Phys. Rev.*, **A24**(1981), 177.
14. L. Sarkadi, *Nucl. Inst. Meth.*, **214**(1983), 43.
15. J. Semaniak, J. Braziewicz, M. Pajek, A. Kobzev, and T. Trautmann, *Nucl. Inst. Meth.*, **B75**(1993), 63.
16. L. Sarkadi and T. Mukoyama, *Nucl. Inst. Meth.*, **B61**(1991), 167.
17. P. Cuzzocrea, E. Perillo, G. Spadaccini, and M. Vigilante, *Nucl. Inst. Meth.*, **B15**(1986), 588.
18. M. Harrigan and D. Cohen, *Nucl. Inst. Meth.*, **B15**(1986), 581.
19. G. Basbas, W. Brandt, and R. Laubert, *Phys. Rev.* **A7**(1973), 983.
20. B. A. Shehadeh, To be published.